A Shear-Wave Seismic System to Look Ahead of a Tunnel Boring Machine

Pawan Bharadwaj, Guy Drijkoningen
Delft University of Technology

Wim Mulder
Shell Global Solutions International BV & Delft University of Technology

Thomas Tscharner
Geo2X

Rob Jenneskens
Seismic Mechatronics

ABSTRACT

The Earth's properties, composition and structure ahead of a tunnel boring machine (TBM) should be mapped for hazard assessment during excavation. We study the use of seismic-exploration techniques for this purpose. We focus on a seismic system for soft soils, where shear waves are better and easier to interpret than compressional waves, as has been shown over the last decade. The system is intended to be deployed on the machine's cutter head, with a few seismic sources and sufficiently many seismic sensors to tackle spatial variability and noise characteristics. An important property of the newly developed system is its ability to process data with very little human interaction. Images need to be available in near real time, without human interactions slowing down the imaging process. This can be achieved by employing Full Waveform Inversion, which minimizes the difference between modeled and observed data. Because this method may suffer from local minima in the cost function if the data lack low-frequency information, we employ a dedicated seismic source that can generate sufficiently low frequencies for the relevant length scales. With data acquired in a number of field settings that mimic realistic TBM configurations, we show that the designed seismic system can successfully look ahead of the TBM and offers a valuable capability to support decision-making during tunnel excavation.

INTRODUCTION

While excavating a tunnel with a Tunnel Boring Machine (TBM), the geology and the ground conditions along the planned tunnel trajectory need to be investigated in order to safely and efficiently carry out the underground operations. This entails detecting the occurrence of boulders, foundations, pipes and faults, necessary to prevent hazards and time-consuming delays in the tunnel boring operations. In order to facilitate ground prediction ahead of a TBM, techniques as used in seismic exploration can be deployed. Two components common to seismic-exploration techniques are data acquisition and processing, the latter including inversion. We will discuss each of these for the application to tunnel excavation with TBM, in particular for soft soils.

Seismic acquisition systems in tunnel exploration

Seismic waves can be generated in the subsurface by either using the TBM cutter wheel itself as source or using specifically designed seismic sources mounted on the TBM. Petronio and Poletto 2002 described a system that uses the cutter-wheel signal. Kneib, Kassel and Lorenz 2000 described a more successful system that uses mounted sources.

Acquisition is usually carried out with a focus on a particular mode of the propagating seismic waves. The use of surface waves was proposed by Bohlen et al. 2007 and Jetschny 2010, considering a system that generates and records tunnel surface waves at the tunnel wall behind the cutter head of the TBM. Compressional or P body waves are commonly used in hydrocarbon exploration. Kneib, Kassel and Lorenz 2000 describes a seismic system for use in soft soil, which uses P-waves up to 6 kHz – higher frequencies than commonly used in existing surface-seismic techniques. The advantage of using shear or S body waves has been demonstrated by several authors in the case of soft-soil near-surface applications (Haines and Ellefsen 2010). Shear waves turn out to be very suitable for soft soils since they are not sensitive to the type of fluid or gas in the pores. Hence, estimated shear-wave properties using shear waves correlate well with subsurface lithology. In these soils, shear waves often have a shorter wavelength than P-waves (Ghose, et al. 1998, Haines and Ellefsen 2010), resulting in better resolution when imaging with shear waves. Also, in the near-surface soft soils where the TBM usually will operate, relative shear-wave variations are much larger than relative P-wave variations. Therefore, we propose a seismic system that uses horizontally polarized shear (SH) waves. For the data acquisition, shear vibrators and receivers are placed on the soil in front of the cutter head to generate and record mainly the SH wave field. Due to the limited space on a TBM, only a limited number of positions for sources and receivers are available, making the imaging more difficult. Our objective is to investigate and demonstrate the feasibility of using SH waves in unconsolidated soils for TBM-like situations and geometries.

Processing techniques used in tunnel exploration

The recorded data are processed to obtain the subsurface parameters that control the seismic wave-propagation process. A *reflectivity* image of the subsurface, which depicts the interfaces between different soil types, can only be produced if a subsurface wave-speed or velocity model is available. The conventional methods of estimating the velocity model directly from seismic data are not fully automatic and require time-consuming human interaction, which may require up to several days to obtain final images. In tunnel-boring operations, this time is not available: results need to be available within an hour or even minutes, to allow for preventive action when obstacles or potentially dangerous situations ahead of the TBM are detected.

Most of the current systems for seismic exploration produce reflectivity images using an assumed velocity model instead of an estimated one. Swinnen, Thorbecke and Drijkoningen 2007 discuss an imaging technique based on focusing operators in an assumed model. Tzavaras 2010 applies Kirchhoff pre-stack depth migration and Fresnel-volume migration to produce 3-D reflectivity images in the case of hard-rock tunnelling. Ashida 2001 describes a method to detect the interfaces using data from multi-component receivers. These conventional near-surface imaging techniques all use an assumed velocity model and suffer from various pitfalls (Steeples and Miller 1998). Incomplete acquisition, due to the limited space on the TBM, causes recording footprint noise in the conventional images. Using an assumed velocity model, which is generally inaccurate, will result in images that are not well focused. Therefore, in tunnelling applications, there is a need for a seismic system that can automatically

estimate the wave-velocity prior to imaging. Bellino, Garibaldi and Godio 2013 propose such a fully automatic method, which can estimate the average wave-velocity as well as the distance to an interface. For the processing and imaging in this paper, we use an approach called Full Waveform Inversion (FWI) (Tarantola 1984, Virieux and Operto 2009), which can automatically produce a subsurface velocity model as well as the corresponding reflectivity image. It requires sufficiently low frequencies in the data to avoid convergence problems, which have been taken care of in the source design. FWI is a nonlinear data fitting procedure that minimizes the misfit between the recorded and modeled seismic data, in our case in a least-squares sense, to estimate the subsurface parameters. The least-squares imaging condition used in FWI will suppress some of the acquisition-related artefacts (Nemeth, Wu and Schuster 1999). Since data need to be processed in near real time with current computing technology, we simplified the SH inversion problem to 2D. We applied a crude but simple correction to the measured 3-D data to make them resemble 2-D data. The 2-D approach implicitly assumes invariance in the out-of-plane direction. In that case, the SH waves are decoupled from P, SV, and Rayleigh waves.

In the remainder of the paper, we first describe the data acquisition of our system and the FWI algorithm applied to the pre-processed data. We then demonstrate its application to synthetic as well as field data. The last section summarizes the paper.

DATA ACQUISITION, PRE-PROCESSING AND INVERSION

Our system places sources and receivers on the soil along a diameter of the cutter head to generate and record seismic shear waves. The system operates when the TBM is stopped. Making use of the rotation of the TBM, different measurements are combined to obtain data along a particular transect, oriented along one of the diameters of the cutter head. The sources and receivers are pushed against the tunnel face to improve the coupling with the soil. Due to the limited space on a TBM, only a few source and receiver positions can be used. We use a vibrator source that can excite signals down to 5 Hz, a low enough frequency for shallow shear-wave surveying. The vibrator source primarily injects a pre-designed signal, often called a sweep, into the ground, perpendicular to the transect. The receivers on the TBM are placed aligned on the cutter wheel of the TBM, and record the vibrations perpendicular to that alignment, thereby recording mainly SH waves.

The recorded data are then pre-processed. Pre-processing includes correction for the pre-designed signal, via a cross-correlation, and also for the receiver instrument response. Since wave propagation in the Earth occurs in three dimensions, the inversion should ideally be done in 3D. However, 3-D inversion is too time-consuming for this TBM application, and therefore a 2-D approach is used in this paper: we assume invariance of the medium parameters in the direction perpendicular to each transect and use a 2-D wave equation. Then an additional approximate correction should be applied to the observed data such that the measured time-domain point-source response (3-D data) is transformed into a line-source response (2-D data). The resulting data after all the corrections are used as input for Full-Waveform Inversion. A quantitative description of the pre-processing steps described above is given in the Appendix.

An important characteristic of Full Waveform Inversion, as part of the total seismic system, is its ability to automatically produce seismic-velocity and/or mass-density maps of the subsurface. The inversion method aims to find one or more unknowns by minimizing the objective function, in our case the least-square error between modeled and observed data. The unknowns in the inversion are the shear wave-speed and mass density, as well as the source- and receiver-coupling functions described in the Appendix. From our experiences in the field, it became obvious that estimation of the coupling

functions is important. For the computation of the modeled SH-wave data, we use a finite-difference scheme to generate modeled data for 2-D heterogeneous models. In the Full Waveform Inversion, the difference between the measured and the modeled data is minimized iteratively, using a non-linear conjugate-gradient scheme. The inputs to FWI are the pre-processed observed data and an initial guess of the velocity and density models. FWI mainly consists of two steps:

1. update seismic shear-wave velocity and/or mass density;
2. update source-coupling and receiver-coupling functions.

RESULTS

Synthetic or Numeric Scenarios

In order to evaluate the performance of FWI in TBM-like settings, some typical scenarios were defined. For each scenario, 2-D synthetic or numeric models are used as an input to a 2-D SH finite-difference wave-equation code that generates synthetic 'observed' data. Table 1 lists the values for seismic shear-wave properties of various subsurface materials as used in the forward modeling. In this section, we present the results of two such scenarios.

For inversion we use a multi-parameter SH full-waveform approach, which means that we invert for both the shear-wave speed and the mass-density. The source filters are also estimated during the inversion. For the recordings, we take the rotation of the TBM into account and combine the measurements at 0 and 180 degrees. Hence, the source and receiver position along a transect are symmetric with respect to the TBM axis. The tunnel axis is assumed to be at a depth of 10 m. The sources and receivers are limited to depths between 5 m to 15 m, thereby assuming a TBM diameter of 10 m (see, e.g., Figure 1).

We consider two acquisition geometries, one rather complete (Geometry 1) and the other taking some practical considerations into account (Geometry 2):

Geometry 1: 5 sources (10 positions) and 20 receivers;

Geometry 2: 2 sources (4 positions) and 18 receivers, noting that: (a) Sources and receivers cannot be placed at the same position. (b) Sources and receivers cannot be placed within a 1-m radius around the center of the cutter head. (c) The minimum distance between a source and receiver is 0.5 m. The source and receiver positions for Geometries 1 and 2 are shown on the TBM of Figures 1 and 2.

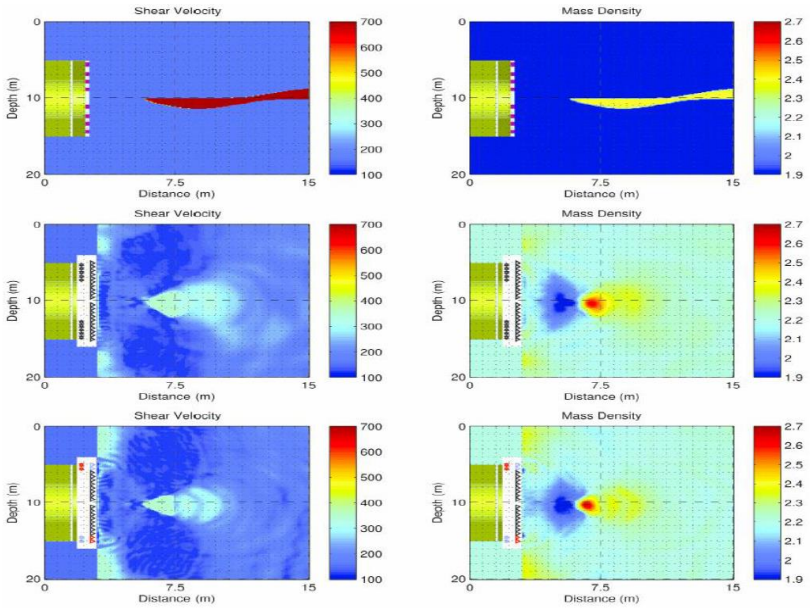

Figure 1. Numeric scenario with an inclusion to test the full waveform inversion algorithm. Assumed shear-wave velocity and mass-density models and final results are shown. Top row: 2D cross section of the inclusion model. Middle: models after FWI inversion using acquisition Geometry 1. Bottom: inverted models using acquisition Geometry 2.

Scenario A: Hard-rock inclusion. In this synthetic case, we used the models shown in at the top row of Figure 1 to generate synthetic observed data. The green box at the left around a depth of 10 m represents the TBM with the cutter head moving to the right. The models represent rock-type inclusion in a soft-soil environment. Often, this type of inclusion is more or less horizontal in young sediments. We take clay as the background medium and limestone as a hard inclusion. The shear-wave velocity of the propagating waves in clay is lower compared to sand or limestone and high frequencies are attenuated due to losses. For that reason, we used a 2–4–140–190 Hz Ormsby wavelet to model the seismic data for a 0.5-s time interval. We only invert the data for the range from 0 to 0.4 s and in the bandwidth between 1 and 190 Hz. We applied multi-scale full waveform inversion, which means that we first invert the low-frequency data and then gradually include higher frequencies. In this case, we first inverted data between 1 and 10 Hz, followed by three bands: 10–20 Hz, 10–50 Hz, and 10–190 Hz.

The middle and bottom rows of Figure 1 show the inversion results using acquisition Geometry 1 and 2, respectively. Ideally, these images should resemble the ground truth of the top row. However, we were only able to image the tip of the inclusion in front of the TBM. This was to be expected since the source cannot illuminate the sides of the inclusion, in such a way that waves would be reflected back to the receivers. It can also be seen that both geometries give nearly equally good results.

Scenario B: Abrupt change. This synthetic case defines a sudden change in geology, for instance, when a compacted sand layer lies next to clay, as is considered next. The top row of Figure 2 shows a 2D cross-section of such a model, again with a part of the TBM drawn on the left in green. Since sources and receivers are positioned in the sand, we used a source with slightly higher frequencies, a 20–40–400–500 Hz Ormsby wavelet, to model the seismic data. We recorded data for 0.5 s but only inverted the first 0.1 s for a source bandwidth of 10–400 Hz. We applied multi-scale full waveform inversion by first inverting the data between 10–30 Hz, followed by three bands: 10–50 Hz, 10–100 Hz, and 10–400 Hz.

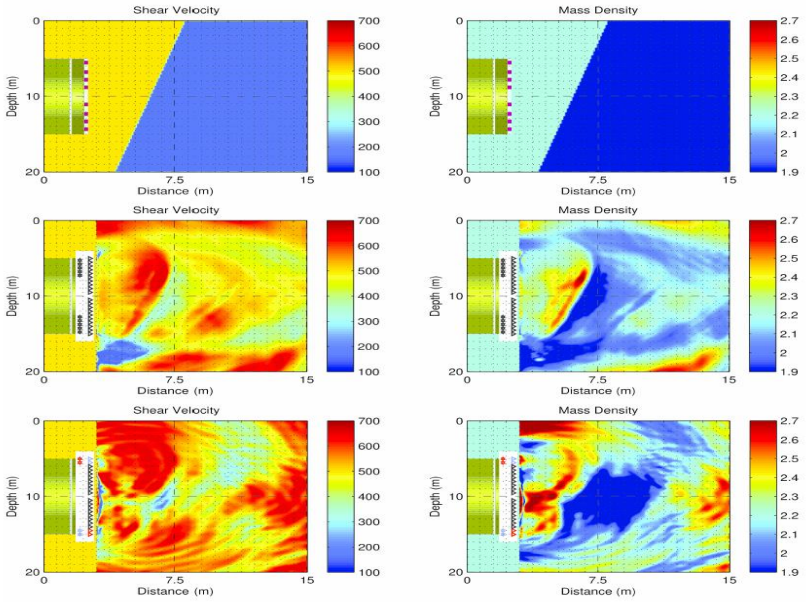

Figure 2. Same as Figure 1, but for the numeric scenario with an abrupt change in geology.

The middle and bottom rows of Figure 2 show the inversion results for acquisition Geometry 1 and 2, respectively. The abrupt change in geology is well imaged with both acquisition geometries, although better with Geometry 1 than with 2. Outside the depth range of 5–15 m, the change is not well imaged and the results are not correct. Interpreting the data outside the region of the TBM trajectory is clearly not reliable. As can be seen for both the reconstructed shear-wave velocity and mass-density models, the results are better for the more complete Geometry 1 than for Geometry 2. This indicates that one should aim for an acquisition with as many sources and receivers as possible.

Table 1. Shear properties of some materials, given as shear-wave velocity and mass-density.

Material	Shear-wave velocity (m/s)	Mass-density (g/cc)
Clay	160	1.8
Sand	500	2.2
Limestone	1300	2.4

Field Scenario

In the previous section, we considered synthetic scenarios as a first step. The next step is to perform tests on field data. These tests were carried out at a site in the Netherlands, where a number of scenarios were built in the field. In these tests, the TBM's assumed direction of advancement was changed to the vertical direction and its progress was simulated by removing layers from surface. The aim was to test the performance of the complete SH-wave system, including the inversion and imaging with FWI, under soft-soil field conditions. To that end, a vertical concrete tube filled with gravel of 1.2 m height and 0.6 m diameter was placed at a depth of $z = 6$ m. The inclusion was buried underneath a 4-m thick package of clay, resulting in an acquisition surface at $z = 2$ m. A surface-seismic experiment mimicking a TBM setting was conducted with 17 receivers, evenly spaced at 0.5 m along two lines on the surface ($z = 2$ m). The two lines were rotated by 60 degrees relative to each other, simulating two stages of a rotating TBM, which is assumed to be stopped during the measurements. For each transect, the coordinate system is rotated such that the x-axis, running from $x = -4$ m to 4 m, is directed along the transect and the y-axis is perpendicular to the transect and advancement directions. The object is located at the center of both transects and is indicated by a red box in the right cross-section of Figures 3 and 4. The receivers measure the out-of-the-plane component, corresponding to the

y-direction, of the particle velocity. We used a shear-wave vibrator that allows us to input a broadband signal into the ground, including the low frequencies as required by FWI to work *automatically*.

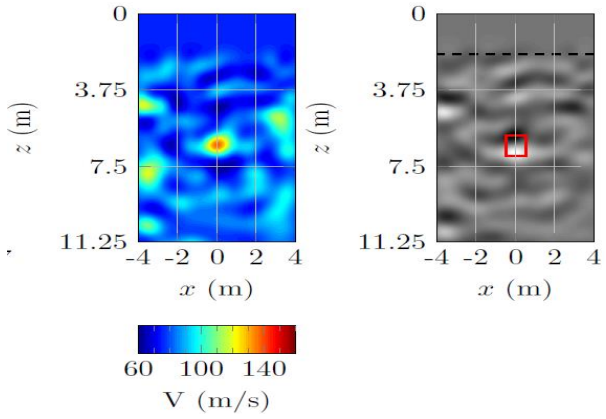

Figure 3. The pre-processed data and inversion results of the first transect. a) Observed shot gather for a source at x = 4 m. b) Modelled shot gather after inversion. c) Estimated shear-wave velocity model of subsurface. d) Image of subsurface depicting the inclusion. The actual location of the inclusion is marked by the red box.

We generated SH waves by placing the vibrator on the surface at the 1^{st}, 3^{rd}, 5^{th}, 13^{th}, 15^{th} and 17^{th} receiver positions. The source signal was a 5 – 120 Hz linear tapered sweep. The photograph in Figure 5 was taken during acquisition and shows the whole set-up.

The pre-processing consisted in applying the correlation with the input sweep, the correction for the amplitude of the receiver's transfer function and the correction for 3-D-to-2-D amplitudes, all according to Equations 2 and 3 in the Appendix. We fitted the recorded shot gathers starting from a homogeneous Earth model with $V = 110$ m/s and $\rho = 1$ gm/cc. The mass-density model is not updated during the inversion and only the data in the bandwidth 50–120 Hz are used. During the inversion, the source related filters, and the receiver coupling factors are estimated, followed by updating the velocity model. After inversion, the modeled data match the observed data quite well. Left columns of Figures 3 and 4 show the final output velocity model for both transects. Note that we are now trying to look downward from the surface, so the images are rotated clockwise by 90 degree compared to the earlier Figures 1 and 2. Right columns of Figures 3 and 4 plot the vertical derivatives of the S-wave impedance models. Applying the derivative boosts the reflectors, the interfaces between different materials where seismic waves are reflected. The results are used for interpretation and we are able to detect a high-velocity anomaly, corresponding to the location of the concrete-tube inclusion. The cause of misplacement of the high-velocity anomaly with an error of about 0.5 m in Figure 4 should be further investigated. This demonstrates the successfulness of our SH-wave seismic system to produce reliable subsurface images, including the possibility to have a fully automatic system.

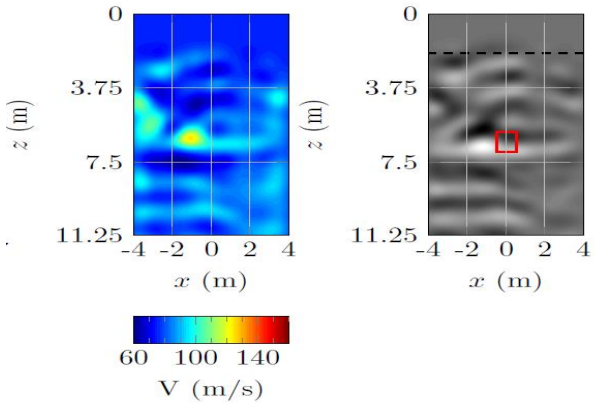

Figure 4. Same as Figure 3, except for the data corresponding to the second transect.

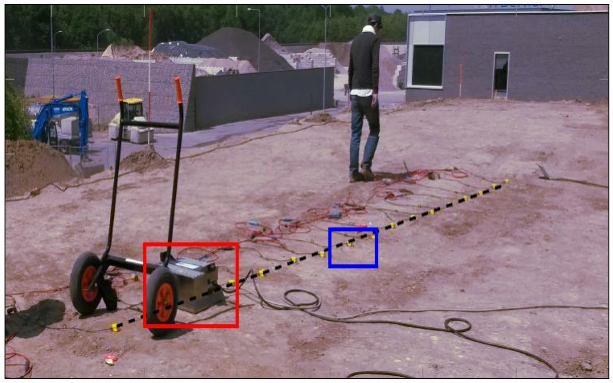

Figure 5. Field acquisition with the shear-wave vibrator (marked by the red box), especially designed for this application, and the receivers (blue box) along a transect (dashed line) similar to what is typical for a TBM situation.

CONCLUSIONS

We propose a ground prediction system that uses horizontally polarized shear-waves for imaging in front of a TBM, in the case of unconsolidated soils. Seismic data are acquired by placing vibrators and receivers on the cutter head of the TBM. The seismic system uses full waveform inversion as imaging engine and can estimate the required shear-wave velocity for subsurface imaging in an automatic way, without human intervention. We investigated the potential of the proposed seismic system using both synthetic and field experiments with TBM configurations. We were able to detect a buried object in the subsurface using FWI. FWI can generate images in a hand-off way and can be used for hazard assessment during TBM drilling in soft soils.

APPENDIX

We give a quantitative description of the acquisition, pre-processing and FWI. The coordinate system has the x-axis always along the transect and the TBM moves into the direction of the z-axis. The vibrator source injects a sweep, $\Phi(\omega)$, as a ground force in primarily the y-direction, perpendicular to the transect. Here, ω denotes the temporal frequency. The inline receivers record only the y-component of particle velocity wave-field. We denote the uncorrelated recorded data at the receivers along a particular transect in the frequency domain by $P_{obs}^{(u)}$, with

$$P_{obs}^{(u)}(x_s, x_r, \omega) = \Phi(\omega) F_s^{(0)}(x_s, \omega) F_r^{(0)}(x_r) I_r(\omega) G_{3D}(x_s, x_r, \omega). \quad (1)$$

In this equation, $F_s^{(0)}(x_s, \omega)$ is a scaling factor that accounts for frequency-dependent ground coupling at a particular source position. Similarly, $F_r^{(0)}(x_r)$ describes coupling at a receiver position and is assumed to be independent of frequency. $I_r(\omega)$ denotes the frequency-dependent receiver's instrument response. G_{3D} is the 3D impulse response of the Earth.

After acquiring the data, a cross-correlation with the source-sweep signal Φ is performed. In the frequency domain, this involves multiplication with its complex-conjugate spectrum. Furthermore, to broaden the bandwidth of the data, a spectral division with the amplitude spectrum of the sweep and the amplitude spectrum of the instrument response is carried out. The frequency-domain correlated data, $P_{obs}^{(3D)}$, are given by

$$P_{obs}^{(3D)}(x_s, x_r, \omega) = \frac{\Phi^*(\omega)\Phi(\omega) F_s^{(0)}(x_s, \omega) F_r^{(0)}(x_r) I_r(\omega) G_{3D}(x_s, x_r, \omega)}{(|\Phi|^2 + \varepsilon_1)(|I_r| + \varepsilon_2)},$$

$$= \frac{\Phi^*(\omega)}{(|\,\Phi\,|^2+\varepsilon_1)(|\,I_r\,|+\varepsilon_2)}\, P_{obs}^{(u)}(x_s, x_r, \omega), \tag{2}$$

where ε_1 and ε_2 are small stabilization factors.
The seismic processing is carried out in two dimensions, so (Wapenaar, Verschuur and Herrmann 1992):

$$p_{obs}^{(2D)}(x_s, x_r, t) = \sqrt{t}\, p_{obs}^{(3D)}(x_s, x_r, t), \tag{3}$$

where $p_{obs}^{(3D)}$ denotes the correlated data in the time domain and $p_{obs}^{(2D)}$ the data after this crude conversion from 3D to 2D. Note that the customary phase correction by $\sqrt{i\omega}$ is skipped and is handled instead by including the source wavelet or filter, treated as an unknown during the inversion. We use $p_{obs}^{(2D)}$ as input to the inversion algorithm.

An important characteristic of this seismic system is its ability to automatically produce velocity and/or mass-density maps of the sub-surface. After they are produced, the *reflectivity* image of the subsurface can be obtained by taking the derivative of the estimated S-wave impedance in the z-direction. FWI is chosen as the method to produce shear-wave parameter maps of the subsurface from the data. The classic least-squares FWI aims to find one or more unknowns by minimizing the objective function,

$$J_{LS} = \sum_s \sum_g \sum_t \left[p_{mod}(V, \rho, x_s, x_r, t) *_t f_s(x_s, t)\, f_r(x_r) - p_{obs}^{(2D)}(x_s, x_r, t) \right]^2, \tag{4}$$

where $*_t$ denotes a convolution operation in time. The unknowns in the inversion are the shear wave-speed V, density ρ, source filters f_s, and the receiver coupling factors f_r. Here, $p_{obs}^{(2D)}(x_r, x_s, t)$ are the correlated observed data, as in Equation 4, for a source at position x_s and receiver at position x_r as a function of time t. The modelled data are denoted by $p_{mod}(V, \rho, x_r, x_s, t)$ and depend on the velocity and density distributions in the subsurface. After inversion, the estimated source filters, f_s, in the frequency domain should be equal to $\frac{\Phi^*(\omega)\,\Phi(\omega)\,I_r(\omega)\,F_s^{(0)}(x_s,\omega)}{(|\Phi|^2+\varepsilon_1)(|I_r|+\varepsilon_2)}$, as in Equation 2. The estimated receiver coupling factors, f_r, should be equal to $F_r^{(0)}$ in Equation 1 after inversion.

Since we adopted a 2-D approximation of the 3-D earth, we assume invariance of the medium parameters in the y-direction of each transect and use a 2-D wave equation. We compute the data by solving the 2-D wave equation, $L\, p_{mod} = f_0$, with $L = \rho \frac{\partial^2}{\partial t^2} - \nabla \cdot \rho V \nabla$. Here, p_{mod} denotes the y-component of the particle velocity, $\nabla = (\frac{\partial}{\partial x}, \frac{\partial}{\partial z})^{\mathrm{T}}$ and f_0 is a source term. For the computation of the synthetic SH-wave data, we use a time-domain staggered-grid finite-difference code (Virieux 1984). This code is also used to compute the gradient of the objective function (Fichtner 2010), as needed for Equation 5 by the optimization scheme.

ACKNOWLEDGEMENTS

This work was carried out as part of the NeTTUN project, funded from the European Commission's Seventh Framework Programme for Research, Technological Development and Demonstration (FP7 2007-2013) under Grant Agreement 280712. The computations were carried out on the Dutch national e-infrastructure with the support of the SURF Foundation (www.surfsara.nl). The first author thanks Jan Thorbecke (TU Delft) for helpful discussions on numerical wave-equation modelling.

WORKS CITED

Ashida, Yuzuru. "Seismic imaging ahead of a tunnel face with three-component geophones." *International Journal of Rock Mechanics and Mining Sciences* (Elsevier) 38, no. 6 (2001): 823-831.

Bellino, Andrea, Luigi Garibaldi, and Alberto Godio. "An automatic method for data processing of seismic data in tunneling." *Journal of Applied Geophysics* (Elsevier) 98 (2013): 243-253.

Bohlen, Thomas, et al. "Rayleigh-to-shear wave conversion at the tunnel face: From 3D-FD modeling to ahead-of-drill exploration." *Geophysics* (Society of Exploration Geophysicists) 72, no. 6 (2007): T67--T79.

Fichtner, Andreas. *Full seismic waveform modeling and inversion.* Springer, 2010.

Ghose, Ranajit, Vincent Nijhof, Jan Brouwer, Yoshikazu Matsubara, Yasuhiro Kaida, and Toru Takahashi. "Shallow to very shallow, high-resolution reflection seismic using a portable vibrator system." *Geophysics* (Society of Exploration Geophysicists) 63, no. 4 (1998): 1295-1309.

Haines, Seth S, and Karl J Ellefsen. "Shear-wave seismic reflection studies of unconsolidated sediments in the near surface." *Geophysics* (Society of Exploration Geophysicists) 75, no. 2 (2010): B59--B66.

Jetschny, Stefan. "Seismic prediction and imaging of geological structures ahead of a tunnel using surface waves." Ph.D. dissertation, Karlsruher Institute of Technologie, 2010, 2010.

Kneib, Guido, Andreas Kassel, and Klaus Lorenz. "Automatic seismic prediction ahead of the tunnel boring machine." *First Break* 18, no. 7 (2000).

Nemeth, Tamas, Chengjun Wu, and Gerard T Schuster. "Least-squares migration of incomplete reflection data." *Geophysics* (Society of Exploration Geophysicists) 64, no. 1 (1999): 208-221.

Petronio, Lorenzo, and Flavio Poletto. "Seismic-while-drilling by using tunnel boring machine noise." *Geophysics* (Society of Exploration Geophysicists) 67, no. 6 (2002): 1798-1809.

Steeples, Don W, and Richard D Miller. "Avoiding pitfalls in shallow seismic reflection surveys." *Geophysics* (Society of Exploration Geophysicists) 63, no. 4 (1998): 1213-1224.

Swinnen, G, JW Thorbecke, and GG Drijkoningen. "Seismic Imaging from a TBM." *Rock Mechanics and Rock Engineering* (Springer) 40, no. 6 (2007): 577-590.

Tarantola, A. "Inversion of seismic reflection data in the acoustic approximation." *Geophysics* 49, no. 8 (1984): 1259-1266.

Tzavaras, Johannes. "3D Tunnel Seismic Imaging." Ph.D. dissertation, Freie Universität Berlin, 2010.

Virieux, J., and S. Operto. "An overview of full-waveform inversion in exploration geophysics." *Geophysics* (SEG) 74, no. 6 (2009): WCC1--WCC26.

Virieux, Jean. "SH-wave propagation in heterogeneous media: velocity-stress finite-difference method." *Geophysics* (Society of Exploration Geophysicists) 49, no. 11 (1984): 1933-1942.

Wapenaar, CPA, Dirk J Verschuur, and Philippe Herrmann. "Amplitude preprocessing of single and multicomponent seismic data." *Geophysics* (Society of Exploration Geophysicists) 57, no. 9 (1992): 1178-1188.